

Supplementary data

Supplementary methods

Purification and characterization of Si-HA by 1H-NMR

Purification steps by dialysis were achieved followed by Si-HA precipitation in 4 °C ethanol 100% and drying at 37 °C for 24h. 1H-NMR spectra of Si-HA polymers were obtained on a Bruker (USA) 400 MHz instrument. 10 mg samples were solubilized in 0.04N NaOD. Spectra were recorded at 80 °C, with a number of scans of NS=64 and a delay DS of 1 s.

HEPES Buffer composition

The buffer composition for Si-HA was the following:

- 336 mM HEPES
- 300 mM NaCl
- 0.22 M HCl

The buffer composition for Si-HPMC was the following:

- 260 mM HEPES
- 310 mM NaCl
- 60 mM HCl

Immunohistochemistry

Immunohistochemistry analyses were performed on 5- μ m thick tissue samples to evaluate the presence of CD68⁺ macrophages. Antigen retrieval was achieved in EDTA buffer (pH 9). Anti-CD68 antibody (abcam 125212, polyclonal rabbit anti-mouse, dilution: 1/1000e) was incubated overnight at 4 °C. A biotinylated secondary antibody (Polyclonal goat anti-rabbit IgG, dilution 1/500e, Dako, USA) was then added for 1 h at room temperature. After signal amplification by Streptavidin-Peroxidase (dilution: 1/400e, Dako, USA), staining was visualized using a DAB kit (Dako, USA). Sections were counterstained using Mayer's hematoxylin. Images were acquired on a whole slide imager and visualized with the NDPview2 software.

Python programs_ Bone evaluation

Briefly, this program was developed with a user interface, allowing the operator to select the pixel chromaticity to be segmented on a drawn line. The average chromaticity underneath the drawn line was computed and pixels values located around this average chromaticity were stored during the segmentation step. A predefined gap around the average chromaticity was set at 40 levels onto the red, green and blue components of the image. The remaining parts (biomaterial, osteoids, soft tissue) were discarded. Bone regeneration was computed within each defect. A similar program was used to specifically segment the osteoids within the full image. To determine the distribution of BCP granules inside the defect, the program was adapted to automatically draw three successive 2-mm-thick concentric rings centered on the Region of Interest, each ring being used to restrict the content of BCP granules within this region. The fraction of BCP granules was finally computed within each ring, from the edge to the center of the biomaterial.

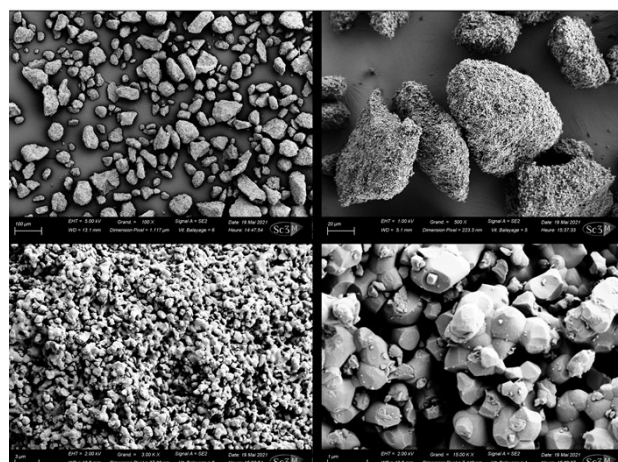


Figure A1. SEM images of MBCP™ granules obtained at different magnifications.

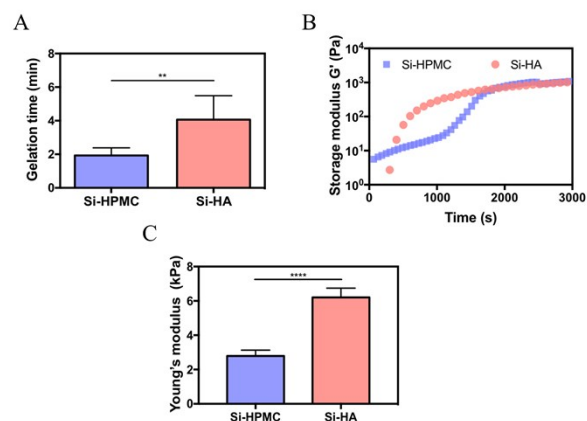


Figure A2. (A) Gelation time of Si-HPMC and Si-HA precursor solutions at 37 °C as determined by multifrequency sweeps, (B), Evolution of the storage modulus of Si-HPMC and Si-HA gels at 37 °C for a constant stress (1 Pa) and frequency (1 Hz), (C) Young's moduli of Si-HPMC and Si-HA gels after 3d of crosslinking at RT.

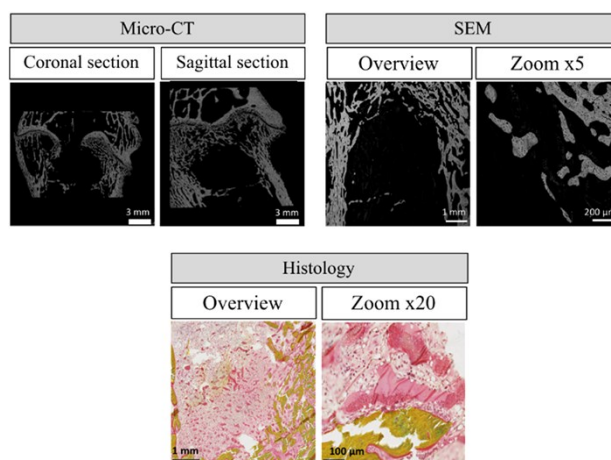


Figure A3. Determination of bone formation within the empty defects using micro-CT, SEM, and histological analyses.

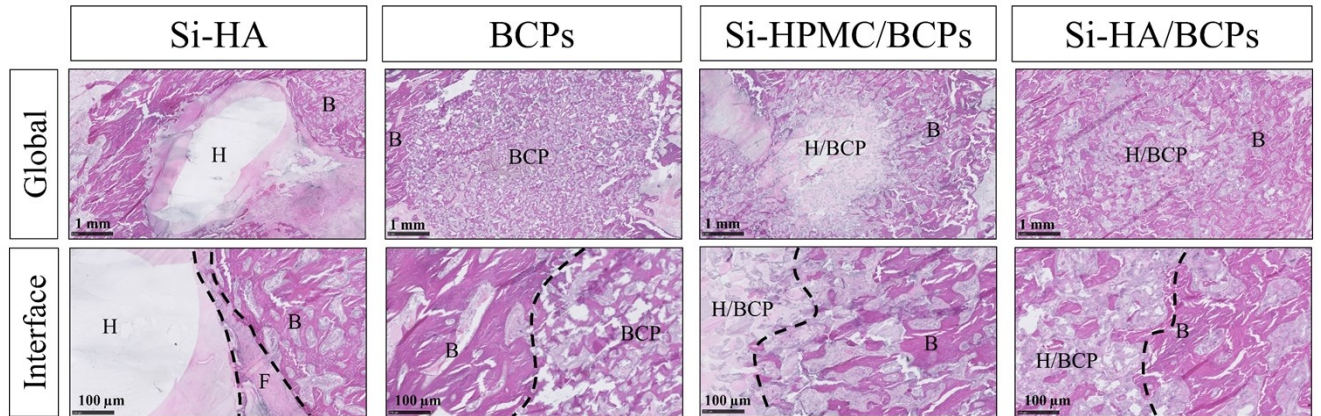


Figure A4. Histological evaluation of defects area by Hematoxylin/Eosin staining at magnification of x1.5 (Global) and x10 (Interface). The dotted line represents the interface between the implant and the mature bone tissue. Abbreviations: B: bone, BCP: BCP granules, F: fibrotic tissue, H: hydrogel, H/BCP: hydrogel + BCP granules.

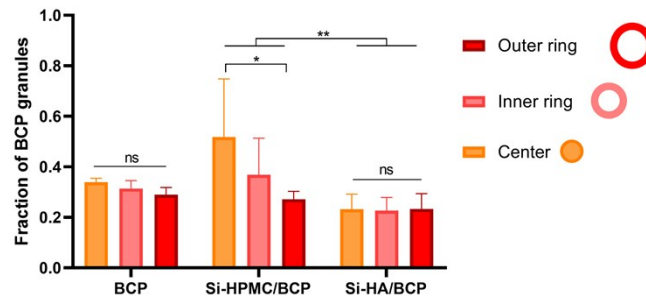


Figure A5. Quantification of the fraction of BCP granules in 3 concentric rings (center: 0-2 mm, inner ring: 2-4 mm, outer ring: 4-6 mm), determined for BCP granules alone, Si-HPMC/BCP and Si-HA/BCP.

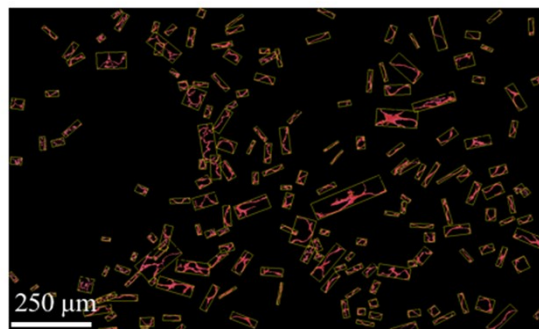


Figure A6. Image processing showing osteoids barrier in a Si-HA/BCP composite. Osteoids (red) are delimited into individual squares (yellow)

